Opportunities for inclusive diffraction at EIC

Wojtek Słomiński (Jagiellonian University)

in collaboration with Nestor Armesto, Paul Newman and Anna Staśto

- Diffractive DIS model and data simulation
- Fits and DPDFs determination vs. HERA
- $F_{\mathrm{L}}^{\mathrm{D}(3)}$ measurement
- $\sigma_{\mathrm{red}}^{D(4)}$ and the subleading contribution study

EIC Yellow Report, 2103.05419
Armesto, Newman, Słomiński, Staśto 1901.09076

XXVIII International Workshop on Deep-Inelastic Scattering and Related Subjects
12-16 April 2021 • Stony Brook, NY

Inclusive diffractive DIS — a résumé

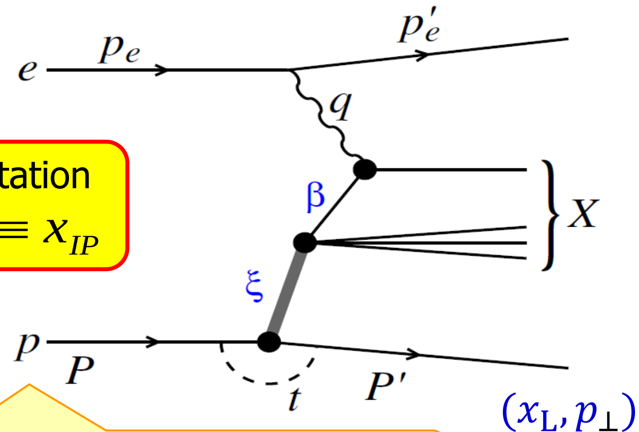

notation
$\xi \equiv x_{IP}$

Proton enters along the $\boldsymbol{z}$ *axis.*

$$\xi \equiv x_{IP} = \frac{(P-P')\cdot q}{P\cdot q} = \frac{Q^2 + M_X^2 - t}{Q^2 + W^2 - m_p^2}$$

$$\beta = \frac{Q^2}{2(P-P')\cdot q} = \frac{Q^2}{Q^2 + M_X^2 - t}$$

$$x = \xi\beta$$

Outgoing proton leaves the interaction region intact, and in a very forward direction.
Its momentum is given in terms of $(x_{\rm L}, \vec{p}_\perp)$ with $P'_+ = x_{\rm L} P_+$.

Cross section • reduced cross section • diffractive structure functions

$$\frac{d\sigma}{d\beta\, dQ^2\, d\xi\, dt} = \frac{2\pi\alpha^2}{\beta Q^4}\left[1 + (1-y)^2\right] \sigma_{\rm red}^{D(4)}(\xi, t, \beta, Q^2)$$

dim = GeV^{-2}

$$\sigma_{\rm red}^{D} = F_2^D - \frac{y^2}{1+(1-y)^2} F_{\rm L}^D$$

Upon integration over t
$\sigma_{\rm red}^{D(3)}, F_{2,L}^{D(3)}$
become dimensionless

Two component model for diffractive SFs (as used in the HERA fits)

Regge factorization works at low ξ (< 0.01).
At higher ξ, subleading exchanges (reggeons/mesons) enter the game — they are all parametrized by a single additional "Reggeon" term

This works within the HERA data accuracy

$$F^{D(4)}(\xi,t,z,Q^2) = \varphi_{\mathbf{P}}(\xi,t)\, F^{\mathbf{P}}(z,Q^2) + \varphi_{\mathbf{R}}(\xi,t)\, F^{\mathbf{R}}(z,Q^2)$$

$\varphi_{\mathbf{P},\mathbf{R}}$ = Regge-type flux:

$$\varphi(\xi,t) = \xi^{1-2\alpha(t)} e^{Bt} \text{ with } \alpha(t) = \alpha_0 + \alpha' t$$

Collinear factorization:

$$F^{\boldsymbol{P}}_{2/\mathrm{L}}(\beta,Q^2) = \sum_k \int_\beta^1 \frac{dz}{z} C_{2/\mathrm{L},\,k}\left(\frac{\beta}{z}\right) f^{\boldsymbol{P}}_k(z,Q^2)$$

Pomeron PDFs obtained via NLO DGLAP evolution starting at μ_0^2 = 1.8 GeV^2 with:

$$f^{\mathbf{P}}_k(z,\mu_0^2) = A_k z^{B_k}(1-z)^{C_k}, \qquad k = g, q$$

$q = d = u = s$

x, Q^2 range — EIC, HERA, LHeC

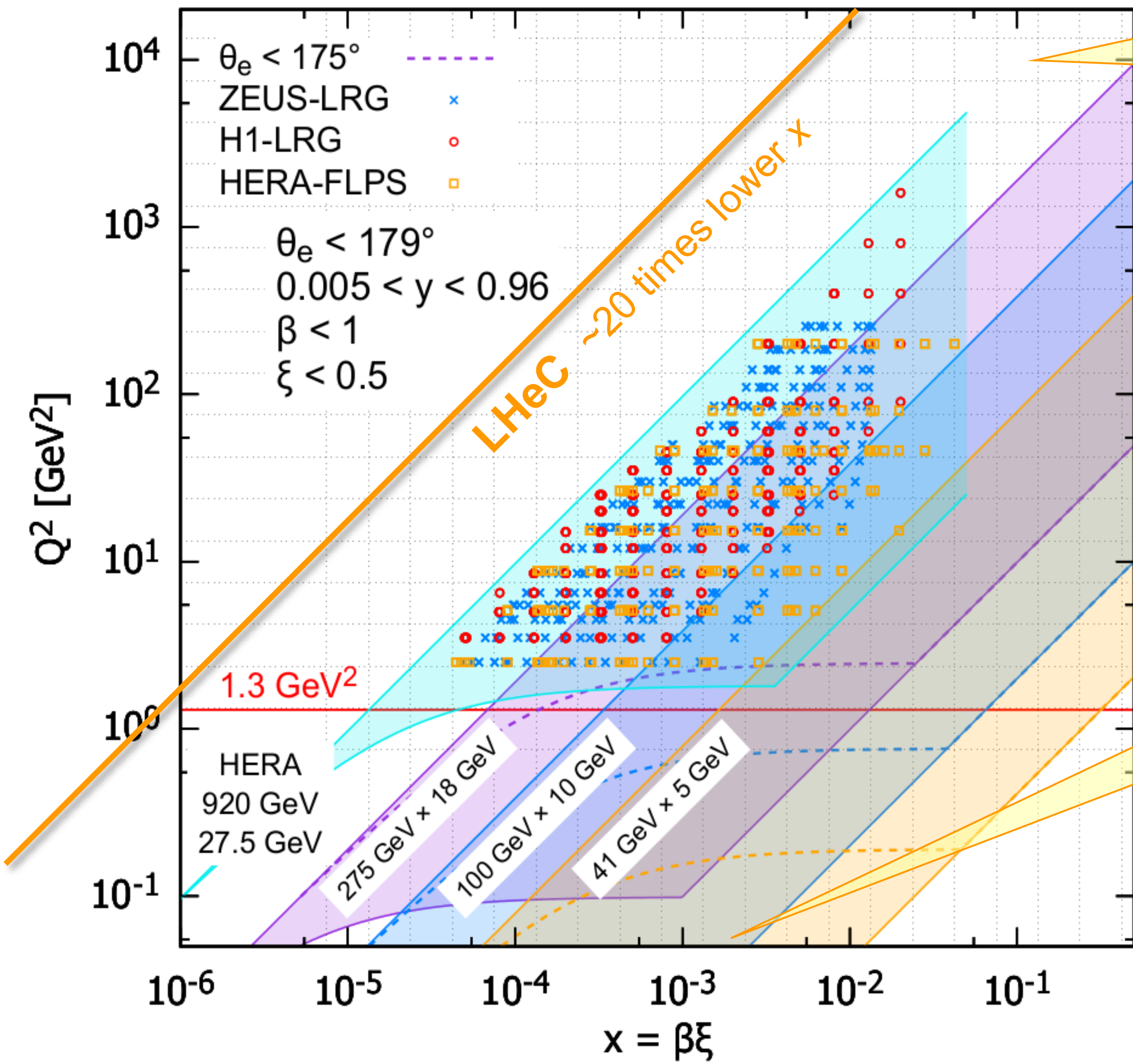

The grid shows binning of 4 bins per order of magnitude in each β, Q^2, ξ

New high x region

x range gets shifted up by a factor ~5 when going from HERA through the EIC beam settings: 18×275, 10×100, 5×41 GeV.

Detailed binning 100x10 275x18

Final proton tagging $-(x_{\mathrm{L}}, t)$ plane

- Very important improvement wrt. HERA
- Cleanest way to select diffractive events

Roman pots	0.5 – 5.0 mrad at 275 GeV
	0.2 – 5.0 mrad at 100 GeV
	1.0 – 4.5 mrad at 41 GeV
B0	6 – 20 mrad

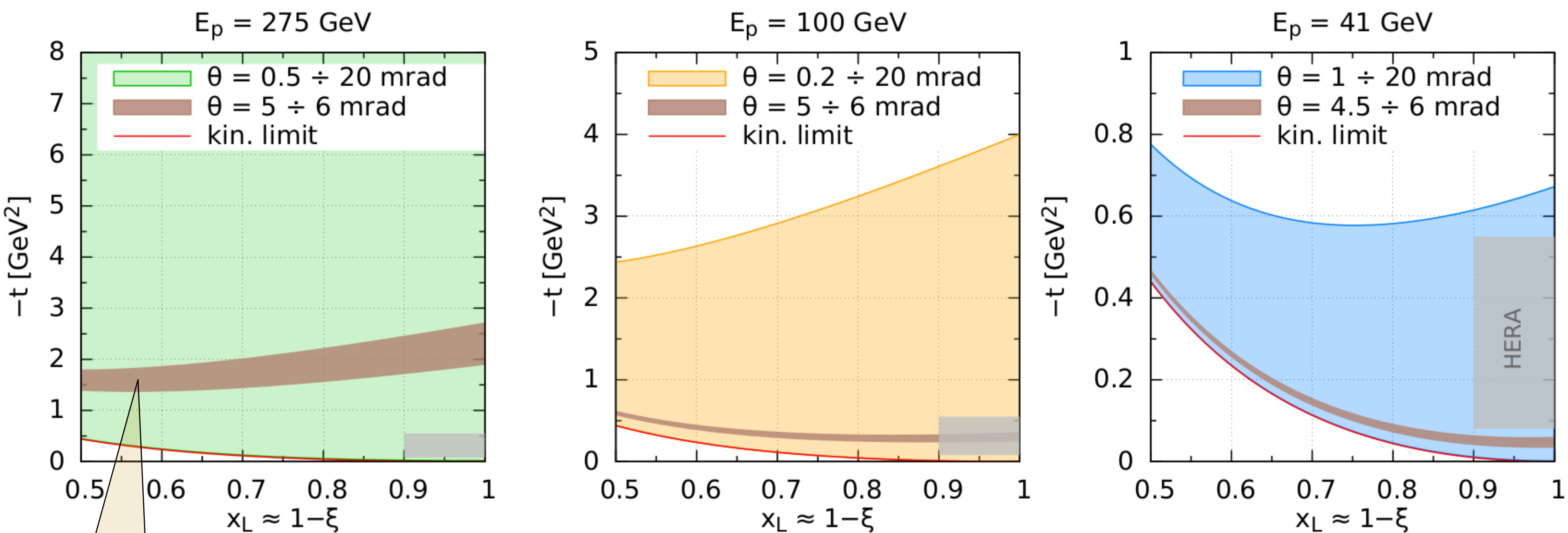

dead zone
~5 – 6 mrad hole
in the EIC detector

$$t = -\frac{p_\perp^2}{x_{\mathrm{L}}} - \frac{(1-x_{\mathrm{L}})^2}{x_{\mathrm{L}}} m_p^2$$

$x_{\mathrm{L}}, p_\perp, \theta$ measured in
LAB = collinear(e,p) frame

DDIS kinematical variables resolution (detector simulations)

Very good resolution for all variables related to $\sigma^{D(3)}$

$E_e = 18$ GeV
$E_p = 275$ GeV

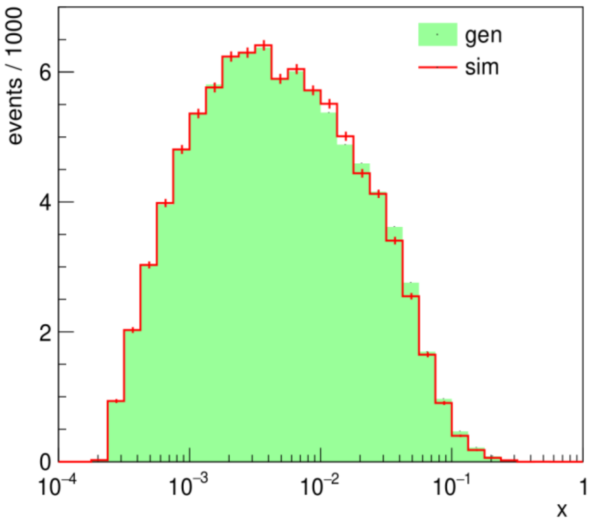

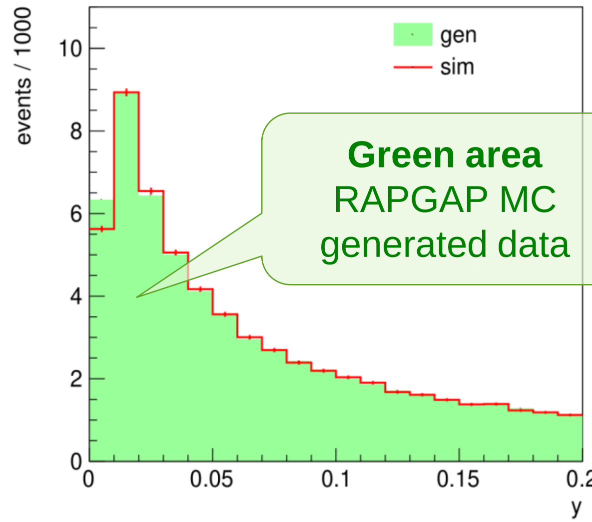

Green area
RAPGAP MC
generated data

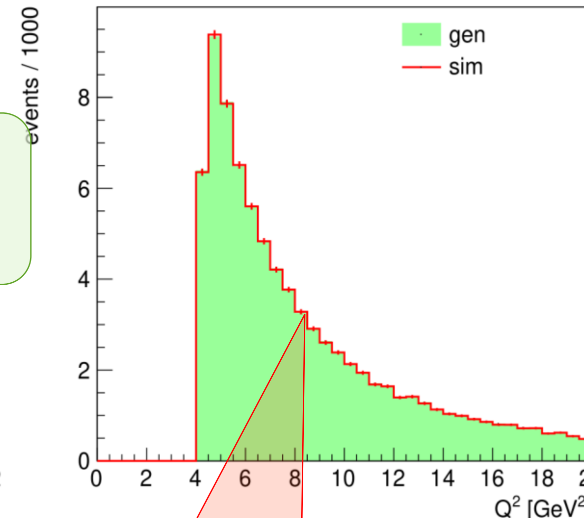

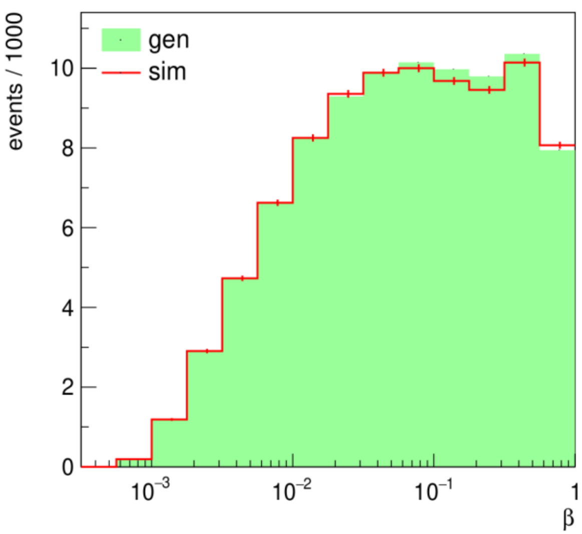

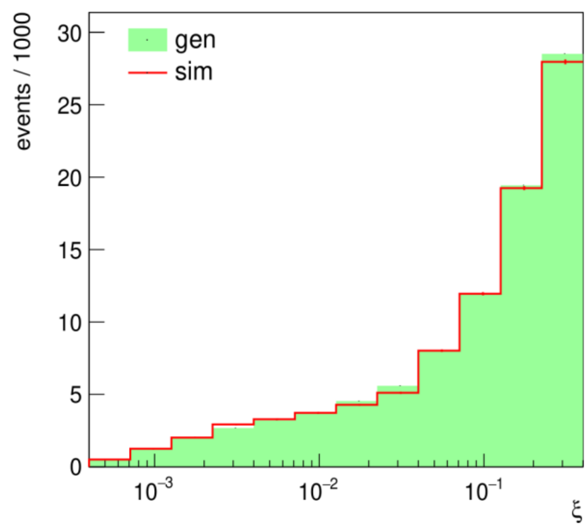

Red histograms
reconstructed from
the detector smeared data

Best reconstruction achieved
by taking average from
several methods
weighted by the resolution

Reconstruction details

Resolution and acceptance for $t, x_L, p_\perp$

$E_e = 18\ \text{GeV}, E_p = 275\ \text{GeV}$

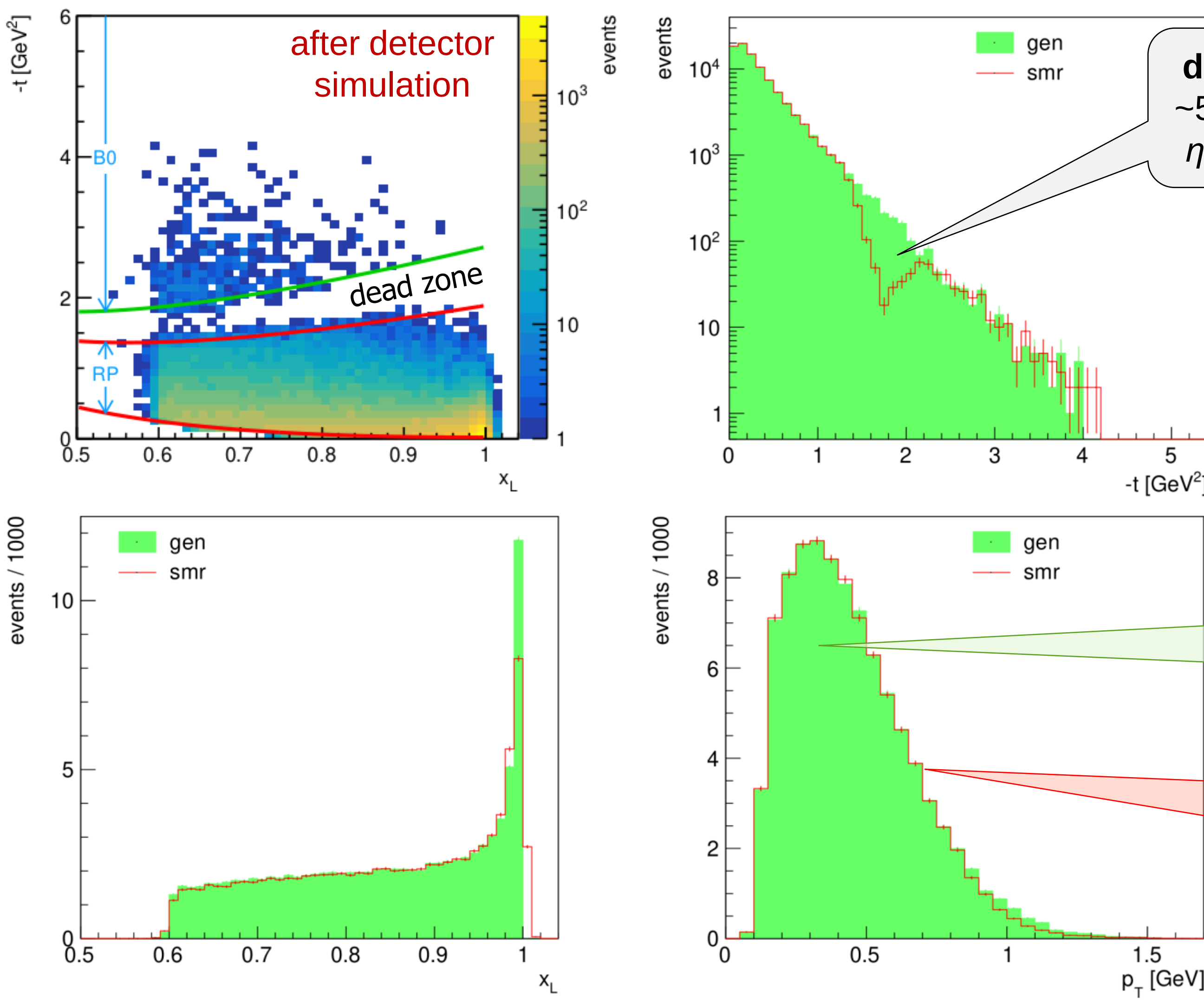

dead zone
~5 – 6 mrad
$\eta = 5.8 - 6$

- Detector design still not absolutely fixed.
- Complementary detector under investigation.

Green area
RAPGAP MC generated data

Red histograms
reconstructed from the detector smeared data

Diffractive PDFs from fits to the $\sigma_{\mathrm{red}}^{D(3)}(\xi, \beta, Q^2)$ data

- Pseudo-data generation
  - Binning:
    - 4 bins per order of magnitude in each β, Q^2, ξ;
    - Very good acceptance and purity
  - Simulations:
    - Extrapolation from ZEUS-SJ DPDFs
    - Random smearing according to $\delta_{\mathrm{sys}} = 5\%$ and δ_{stat} from 10 fb^{-1} integrated luminosity; errors are dominated by systematics
  - Several random samples generated

- DPDFs fits to $\sigma_{\mathrm{red}}^{D(3)}$
  - Out of all 13 parameters:

$$f_g^{\mathbf{P}}(z, \mu_0^2) = A_g z^{B_g}(1-z)^{C_g}$$

    - 4, $B_{P/R}, \alpha'_{P/R}$ are fixed from other measurements, *e.g.* $\sigma_{\mathrm{red}}^{D(4)}$
    - 9 remain to be fitted → Standard fit — Fit S
    - Option: constant gluon at μ_0^2, i.e. $B_g = C_g \equiv 0$ → Fit C with 7 parameters

$\sigma_{\rm red}^{D(3)}$ pseudo-data examples

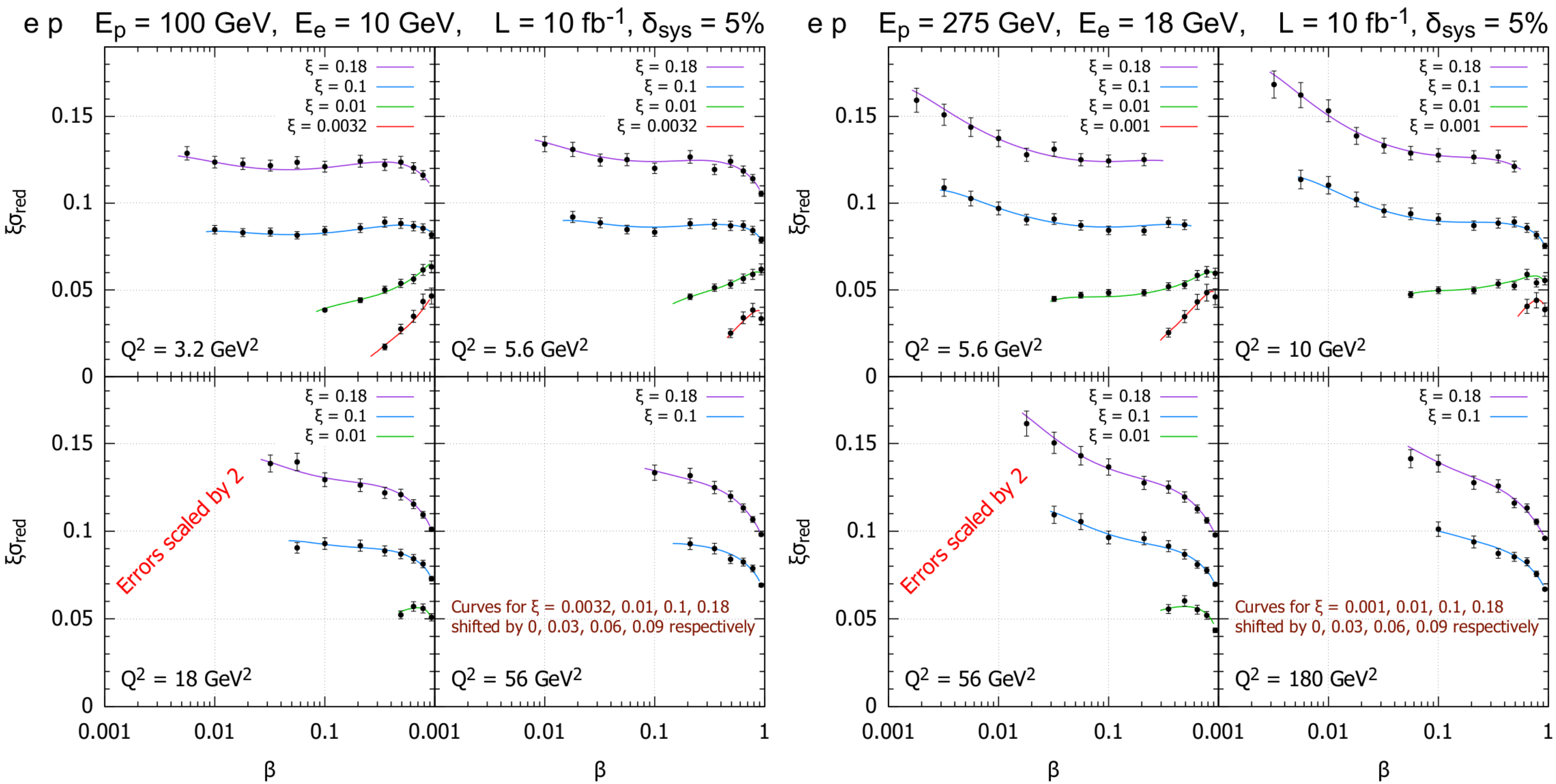

In total:
482 points for $1.3 < Q^2 < 1330\ \mathrm{GeV}^2$

In total:
792 points for $1.3 < Q^2 < 4220\ \mathrm{GeV}^2$

Very precise data

Quark and gluon DPDFs from fits to 18 GeV × 275 GeV data

quark

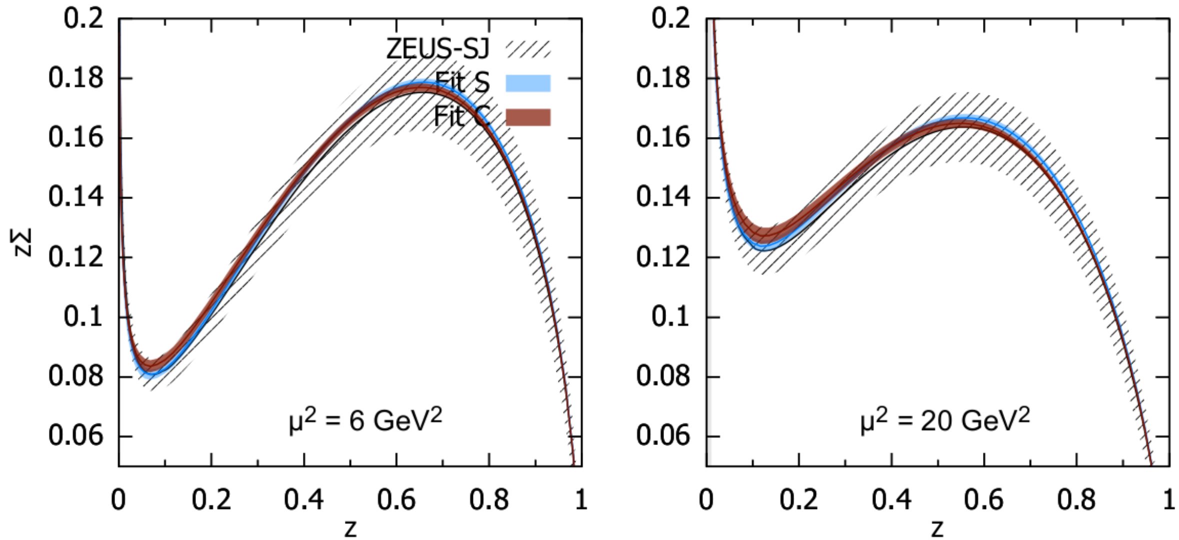

gluon

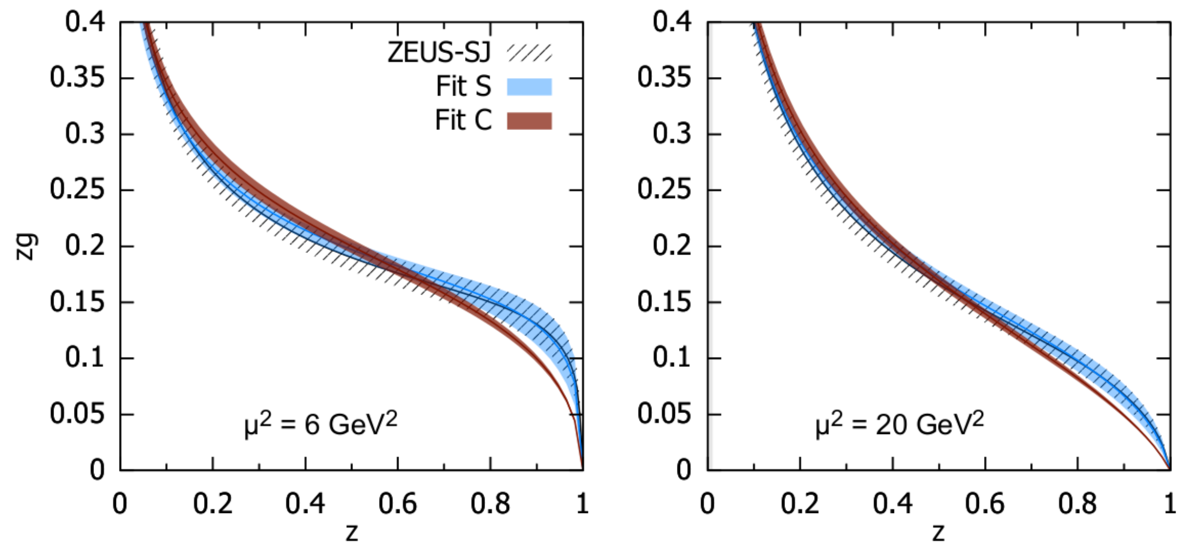

Data selection
$Q^2 > 5\ \mathrm{GeV}^2$, $\xi < 0.1$
375 data points

- Fit S: 9 parameters,
- Fit C: 7 parameters:
  $B_g = C_g \equiv 0$

As compared to HERA

- Much smaller uncertainty for the quark DPDF at high z
- No improvement for gluon
  - Both S and C fits give $\chi^2 \approx 1$
  - Another, gluon-sensitive process needed, e.g. dijet production, dominated by BGF

Inclusive diffraction on nuclei — simulations for gold

Nuclear shadowing & diffraction are related

- High accuracy
- No model to fit

Nuclear modification factors from the Frankfurt-Guzey-Strikman model, Phys. Rep. 512, 255 (2012)
Two scenarios for high (H) and low (L) shadowing considered.

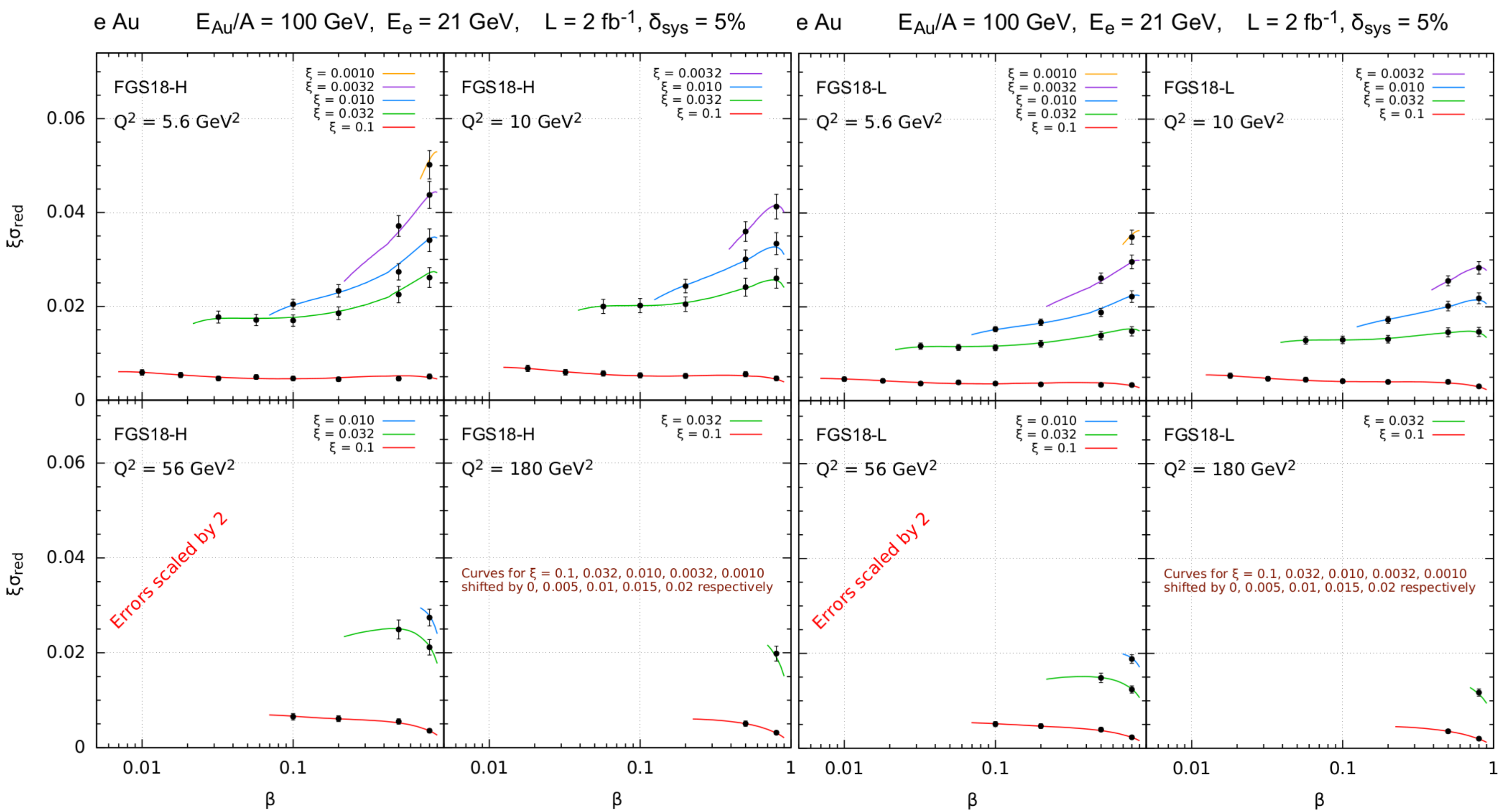

Extrapolation — Pomeron, Reggeon, F_2, F_L components of $\sigma_{\text{red}}^{D(3)}$

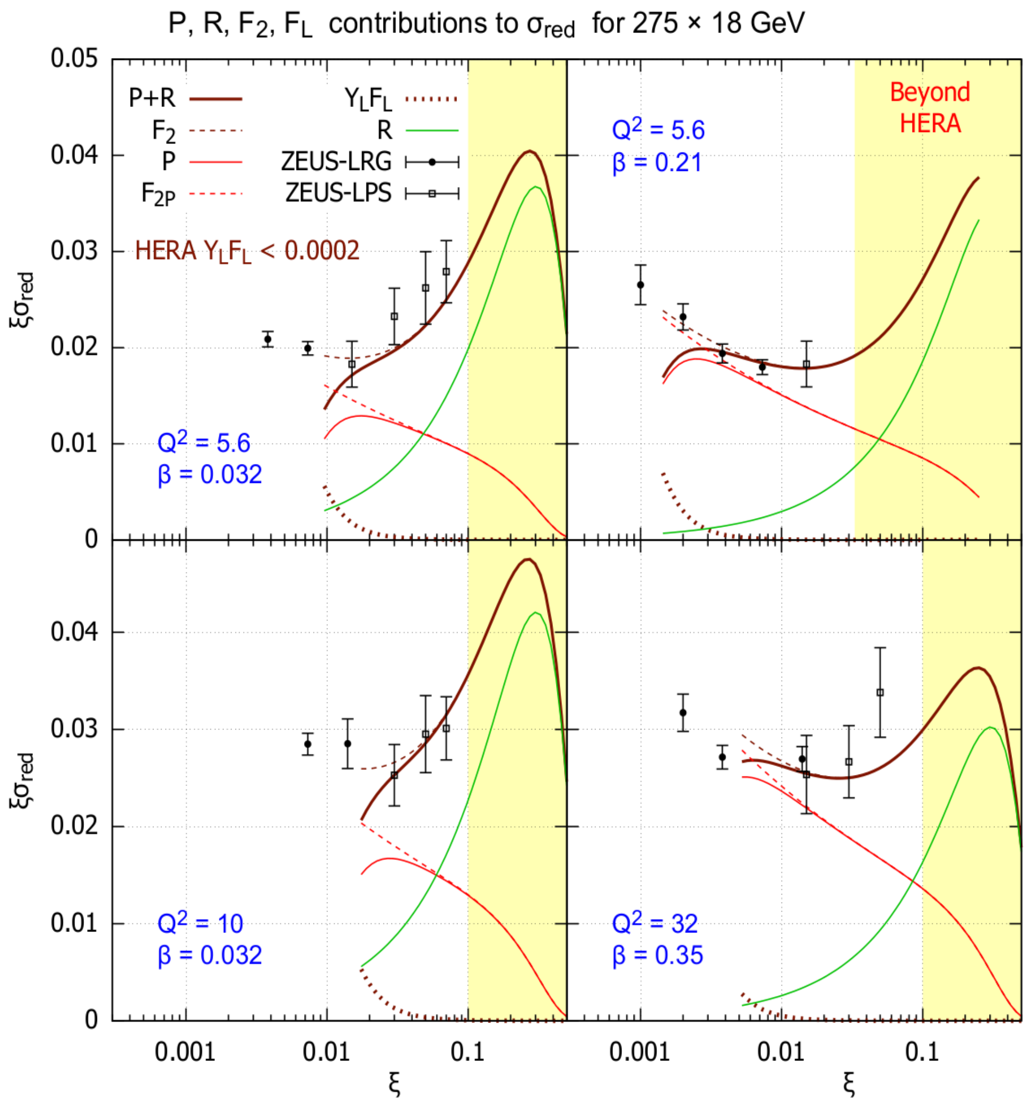

$E_e = 18$ GeV, $E_p = 275$ GeV

- Pomeron dominates at low ξ, — especially at higher β
- "Reggeon" contribution grows with ξ
  - Dominates for $\xi > 0.1$
  - High ξ region accessible by the final proton tagging at EIC

$$\sigma_{\text{red}} = F_2 - \frac{y^2}{1+(1-y)^2} F_L$$

- Significant F_L component, ~30 times higher than at HERA due to higher y values

$F_{\mathrm{L}}^{\mathrm{D}(3)}$ investigation

Challenging but not impossible

- 18 beam setups used for the simulations:

  $E_e \times E_p$ = {5, 10, 18} × {41, 100, 120, 165, 180, 275} GeV

- $\delta_{\mathrm{sys}} = 2\%$ and δ_{stat} from $10\ \mathrm{fb}^{-1}$ integrated luminosity

- 469 bins in (ξ, β, Q^2) selected such that
  - contain at least four σ_{red} data points
  - $Q^2 > 3\ \mathrm{GeV}^2$,
  - $M_X > 2\ \mathrm{GeV}$.

- F_2, F_{L} obtained from fits to σ_{red} vs. Y_{L}:

$$\sigma_{\mathrm{red}} = F_2\ (\xi, \beta, Q^2) - Y_{\mathrm{L}}\ F_{\mathrm{L}}\ (\xi, \beta, Q^2)$$

separately in each (ξ, β, Q^2) bin

$$Y_{\mathrm{L}} = \frac{y^2}{1 + (1-y)^2}$$

$$y = \frac{Q^2}{\xi \beta s}$$

Simulated measurement of $F_L^{D(3)}$ vs. β in bins of (ξ, Q^2)

Example results of F_L fitted to $\sigma_{red} = F_2 - Y_L(y)\, F_L$

76 bins in (ξ, Q^2)

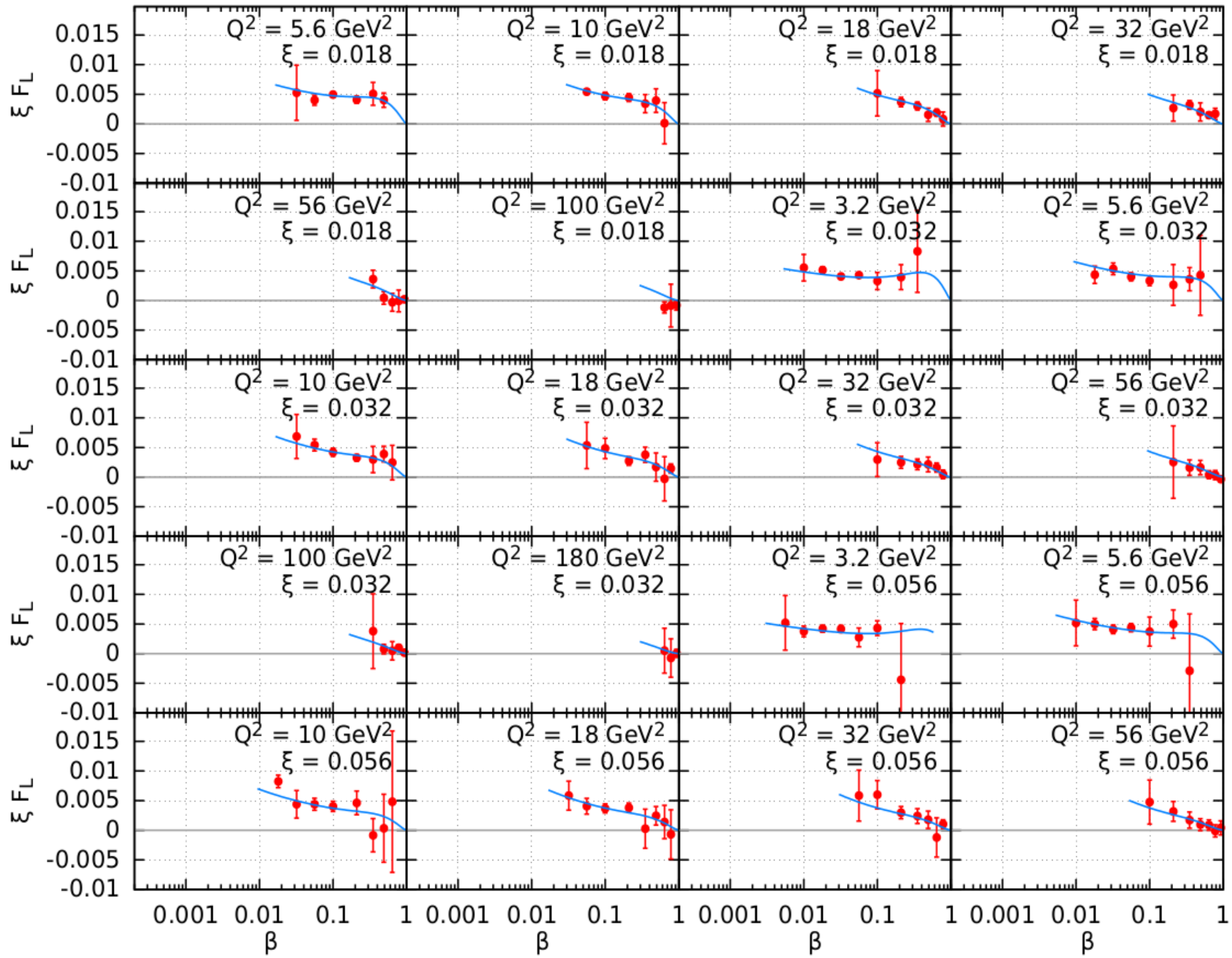

20 bins shown

F_L fit

F_L model

Error bars correspond to the 90% confidence interval.

A reliable measurement of $F_L^{D(3)}$ within the reach of EIC

$\sigma_{\rm red}^{D(4)}$ vs. (ξ, t) simulations

From the ZEUS-SJ fit

$$\xi \varphi_P(\xi, t) \propto \xi^{-0.22}\, e^{-7|t|}$$

$$\xi \varphi_R(\xi, t) \propto \xi^{0.6+1.8|t|}\, e^{-2|t|}$$

Pomeron and "Reggeon" components have very different shapes in ξ and t

- Extrapolation of $\sigma_{\rm red}^{D(4)}(\xi, t, \beta, Q^2)$ calculated using ZEUS-SJ DPDFs
- Simulation done by random smearing according to
  - $\delta_{\rm sys} = 5\%$
  - $\delta_{\rm stat}$ from $L = 10\ {\rm fb}^{-1}$

Nb. statistical errors increase at large |t|

Simulations for $\sigma_{\mathrm{red}}^{D(4)}$ vs. t

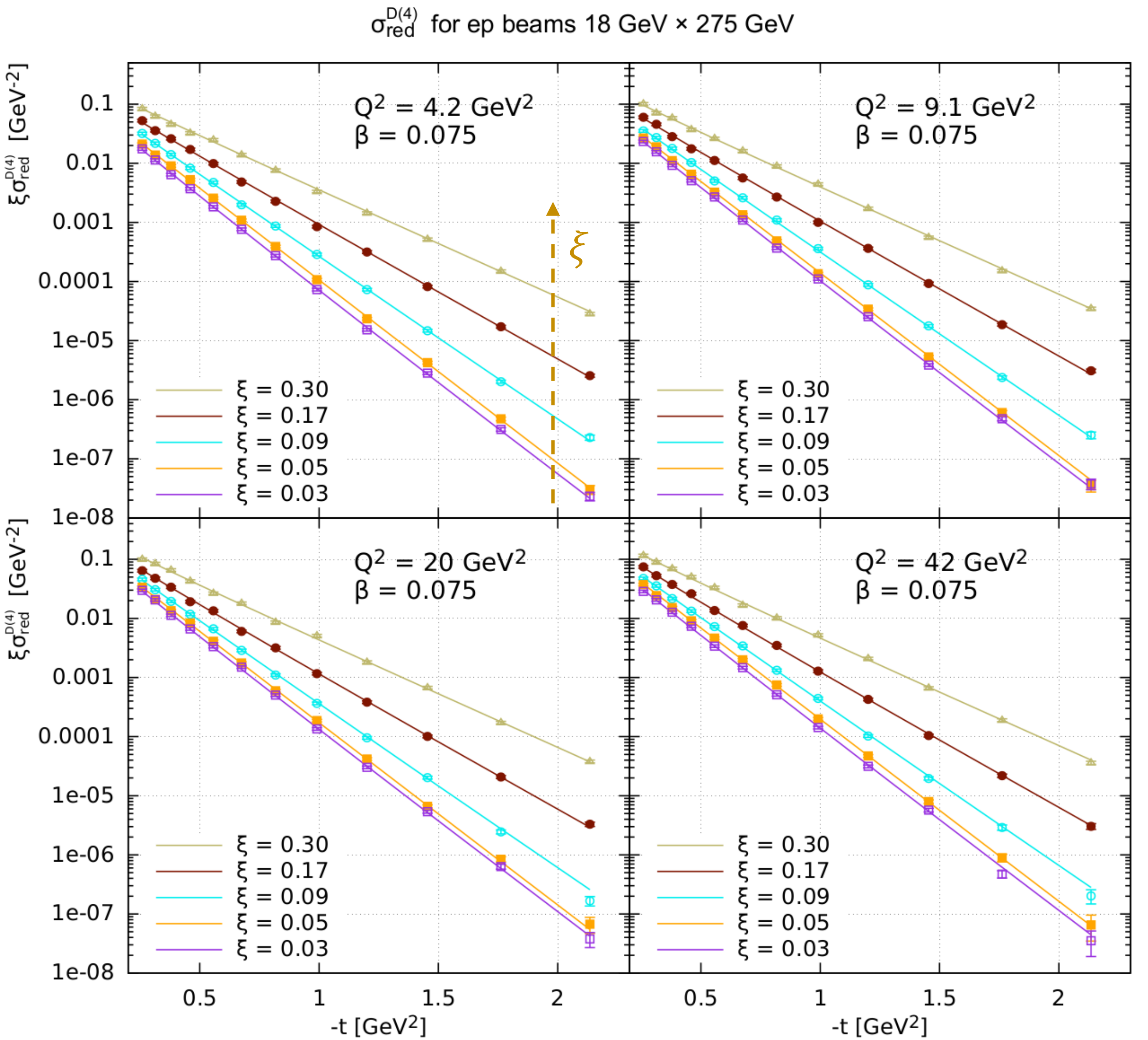

$E_e = 18$ GeV
$E_p = 275$ GeV

Lines — extrapolation
Points — simulation

$$C_P\,\xi^{-0.22}\,e^{-7|t|} + C_R\,\xi^{0.6+1.8|t|}\,e^{-2|t|}$$

Very well measurable t-slope vs. ξ

Simulations for $\sigma_{\text{red}}^{D(4)}$ vs. ξ

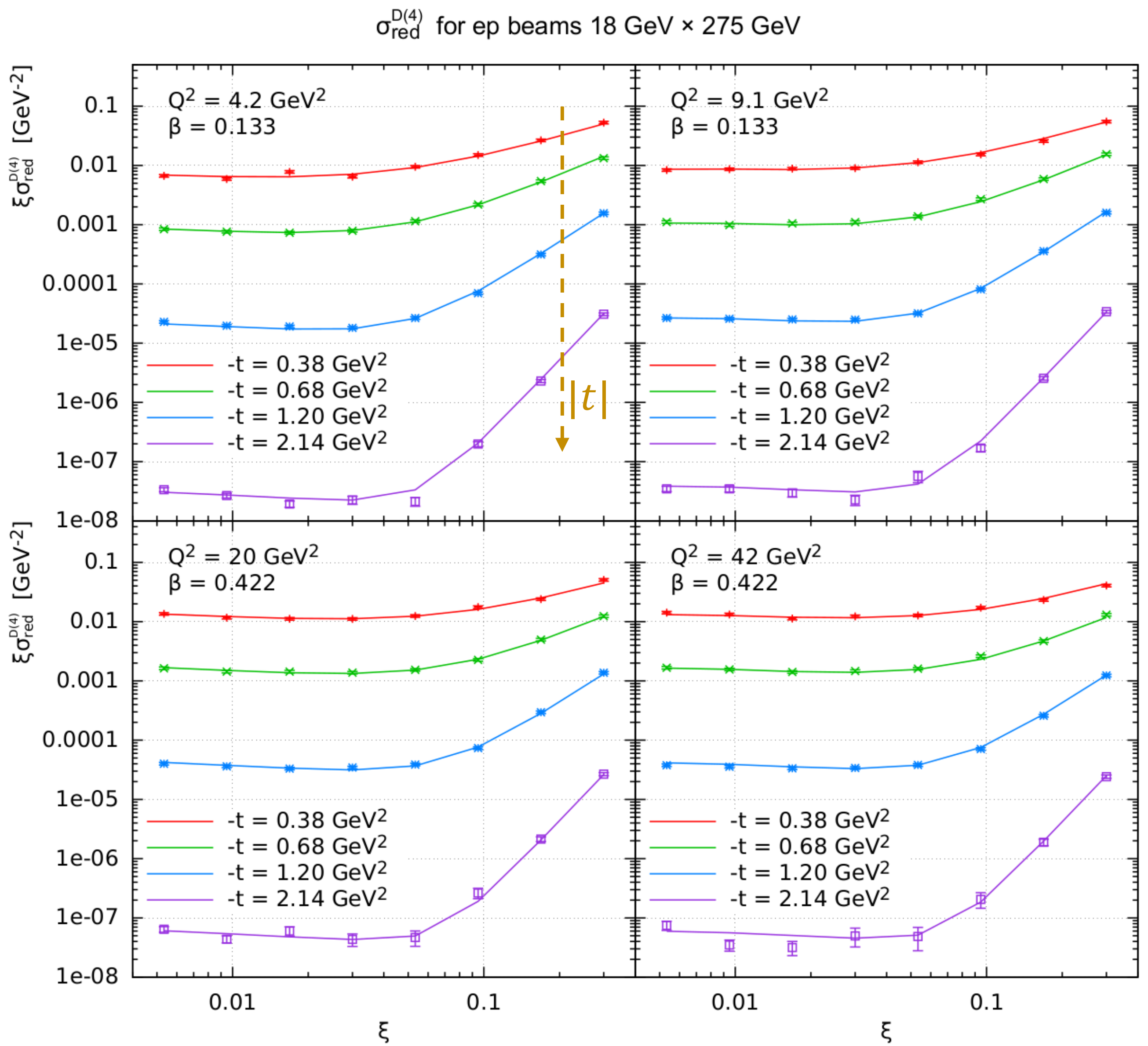

$E_e = 18$ GeV
$E_p = 275$ GeV

Lines — extrapolation
Points — simulation

$$C_P\, \xi^{-0.22}\, e^{-7|t|} + C_R\, \xi^{0.6+1.8|t|}\, e^{-2|t|}$$

Very well measurable dependence on ξ

Double-slope structure?

Summary

❑ EIC detector capabilities

- ❑ Powerful final proton tagging
- ❑ Very good acceptance and resolution for the diffractive DIS variables

❑ Prospects

- ❑ Precise *e-p* and *e-A* $\sigma_{\mathrm{red}}^{D(3)}$ measurements
- ❑ Pomeron PDFs extraction — high accuracy for quarks at high β
- ❑ $F_{\mathrm{L}}^{D(3)}$ determination in wide range of (ξ, β, Q^2)
- ❑ Precise *e-p* $\sigma_{\mathrm{red}}^{D(4)}$ vs. (ξ, t) measurement down to $x_{\mathrm{L}} \approx 0.6$
  - ❑ Subleading "Reggeon" contribution
  - ❑ "Leading proton" region

BACKUP

Detailed binning 100 × 10 GeV

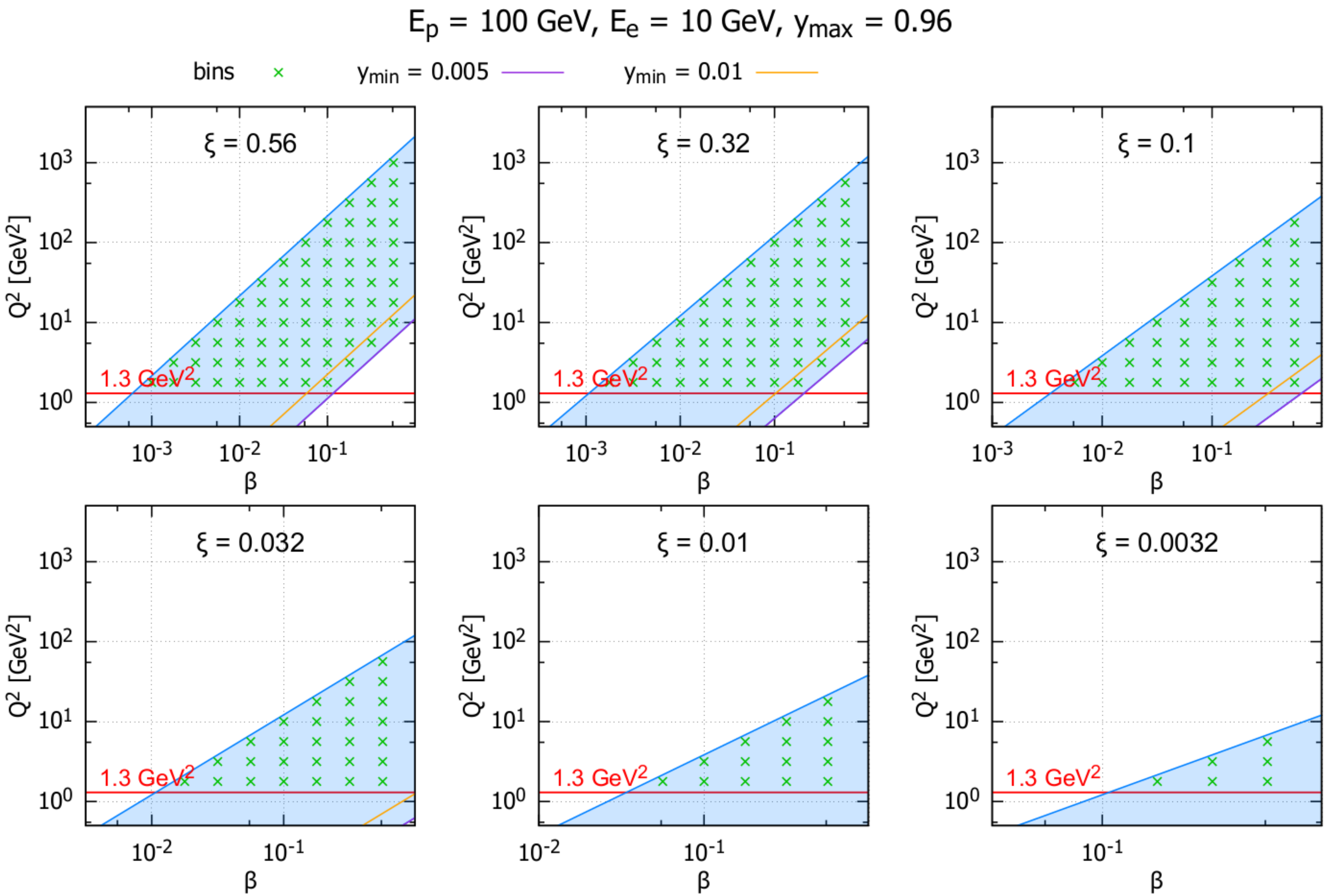

Detailed binning 275 × 18 GeV

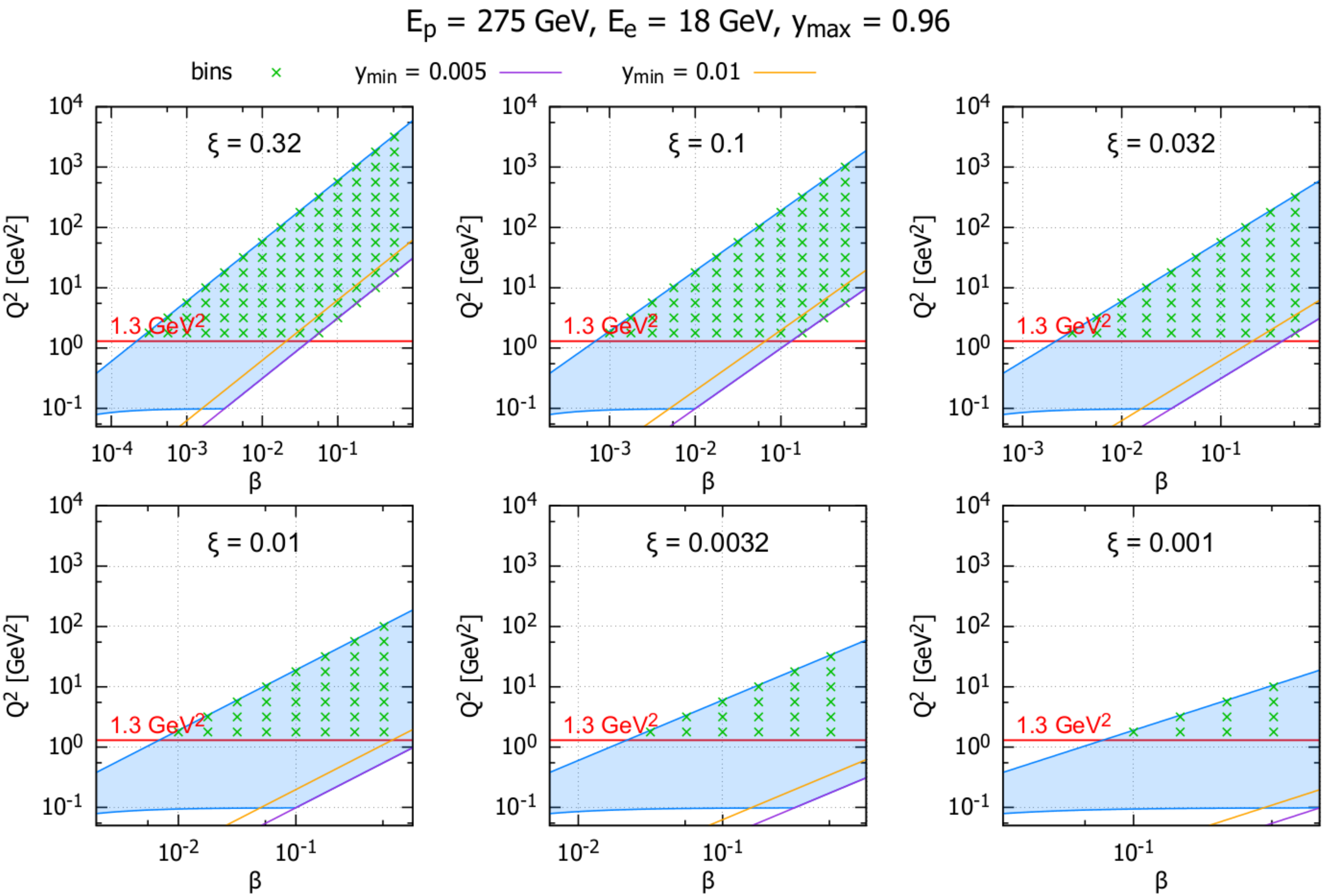

Reconstruction of kinematic variables

Several methods of kinematical reconstruction are used to produce the final values as averages weighted by the experimental resolution.

- Q^2, x, y by weighted average of
  - "Electron" and "Double angle" methods
- Additionally, M_X, β, ξ by weighted average of
  - MX method:
    - $M_X = P_X^2$ (from all EFOs)
    - $\beta = \frac{Q^2}{Q^2+M_X^2-t}, \ \xi = \frac{x}{\beta}$
  - MP method:
    - $\beta = \frac{Q^2}{2(P-P')\cdot q}$
    - $M_X = \frac{1-\beta}{\beta} Q^2 + t, \ \xi = \frac{x}{\beta}$

Rapidity gap

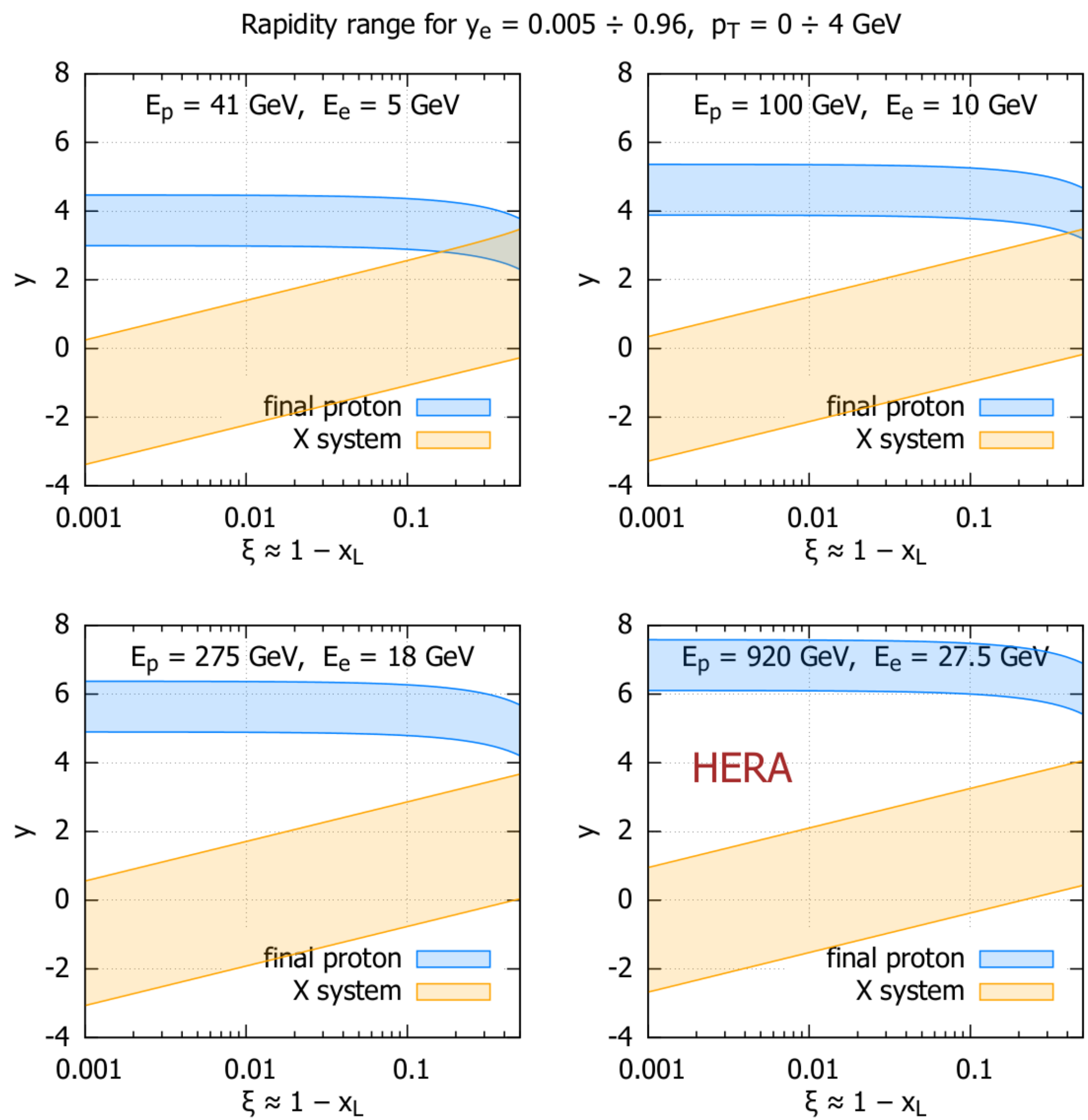

Rapidity gap

- grows with s
- shrinks $\sim \ln\frac{1}{\xi}$

Pseudo-rapidity distribution

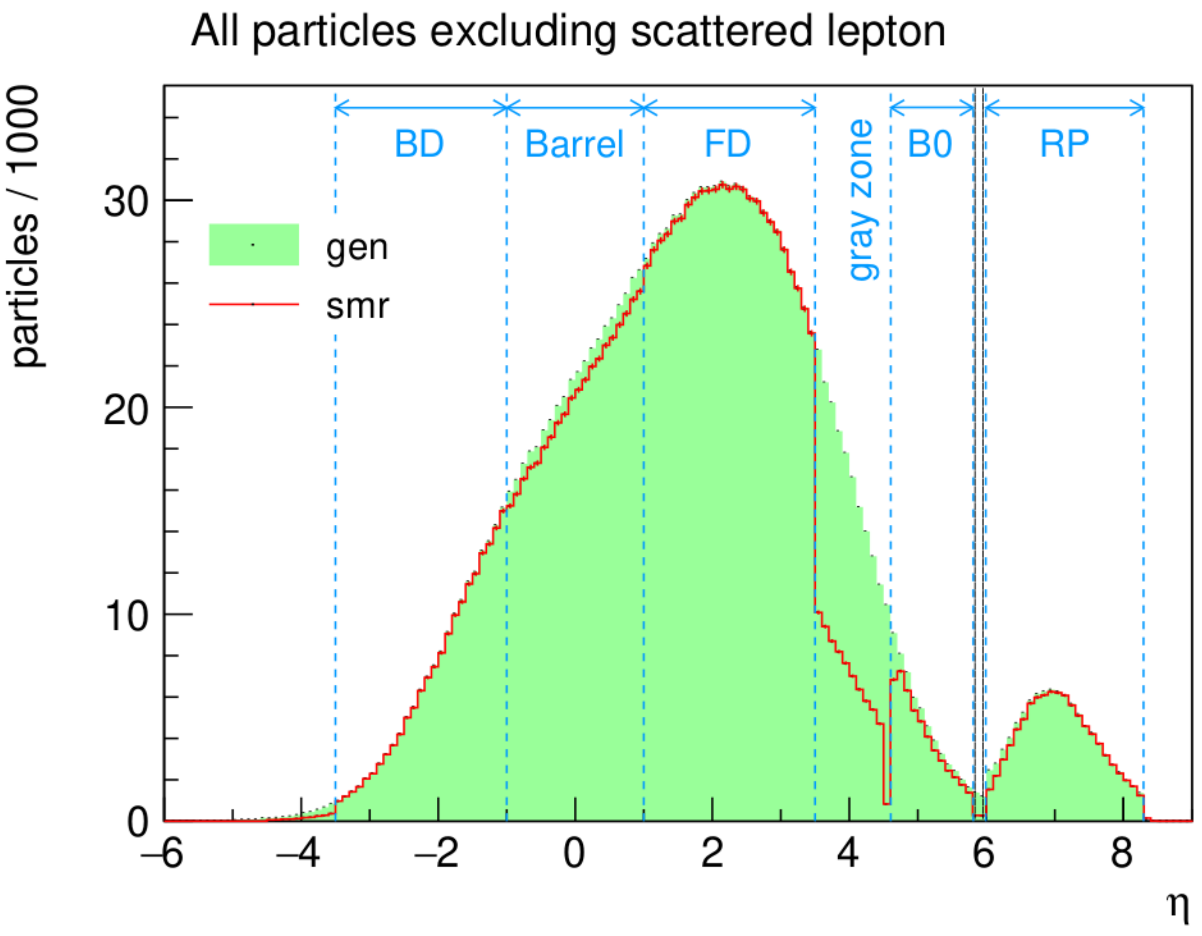

gray zone
covered by
EMCAL only

Gluon DPDFs form C and S fits

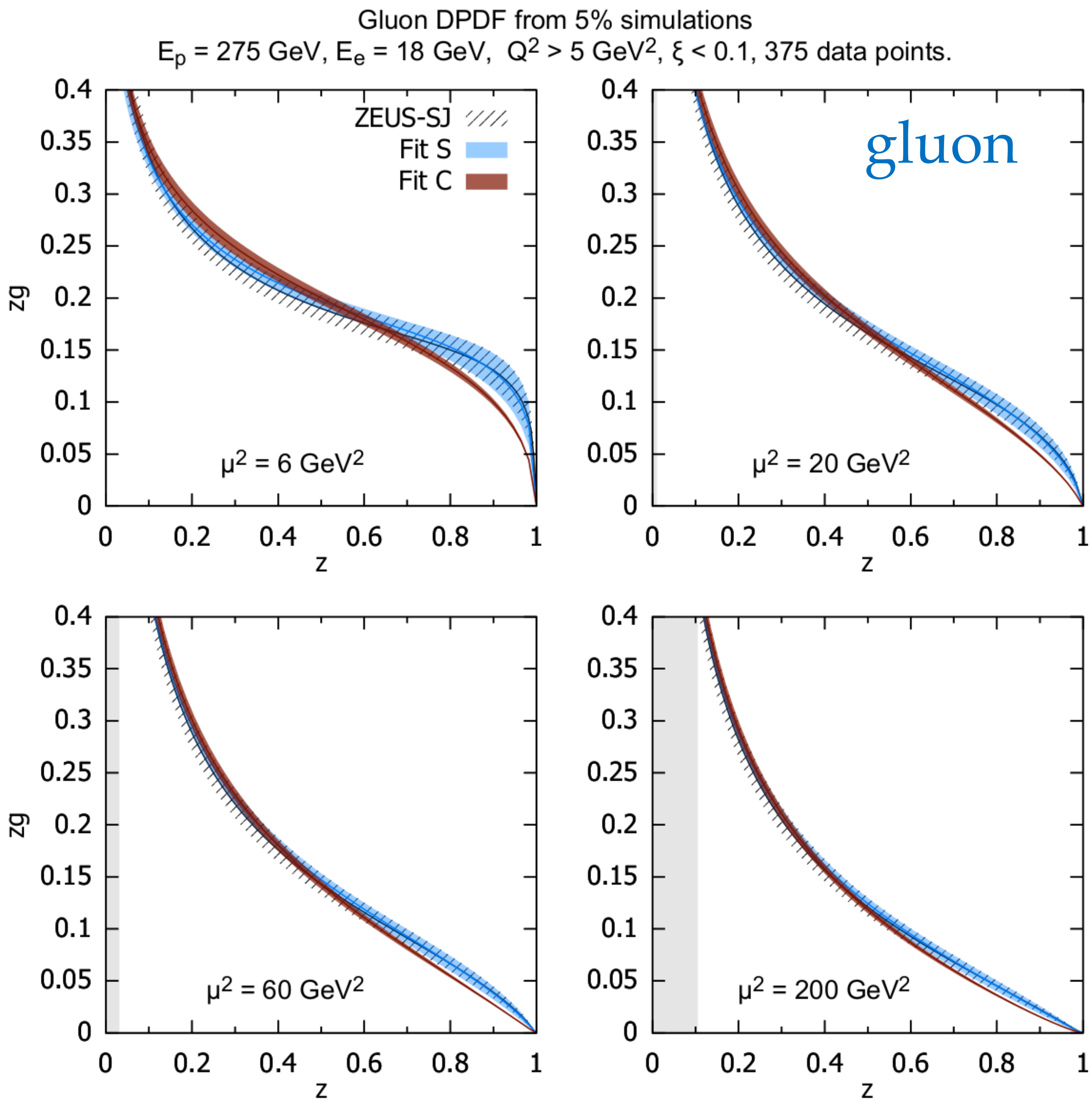

Data selection
$Q^2 > 5\ \mathrm{GeV}^2$
$\xi < 0.1$
➔ 375 data points

- ❑ Both C and S fits give $\chi^2 \approx 1$
- ❑ Fixing gluon from inclusive DDIS requires $x \lesssim 10^{-6}$
- ❑ Here $x > 10^{-4}$
- ❑ Some other, gluon-sensitive process needed – e.g. dijet production, dominated by BGF

Quark DPDFs form C and S fits

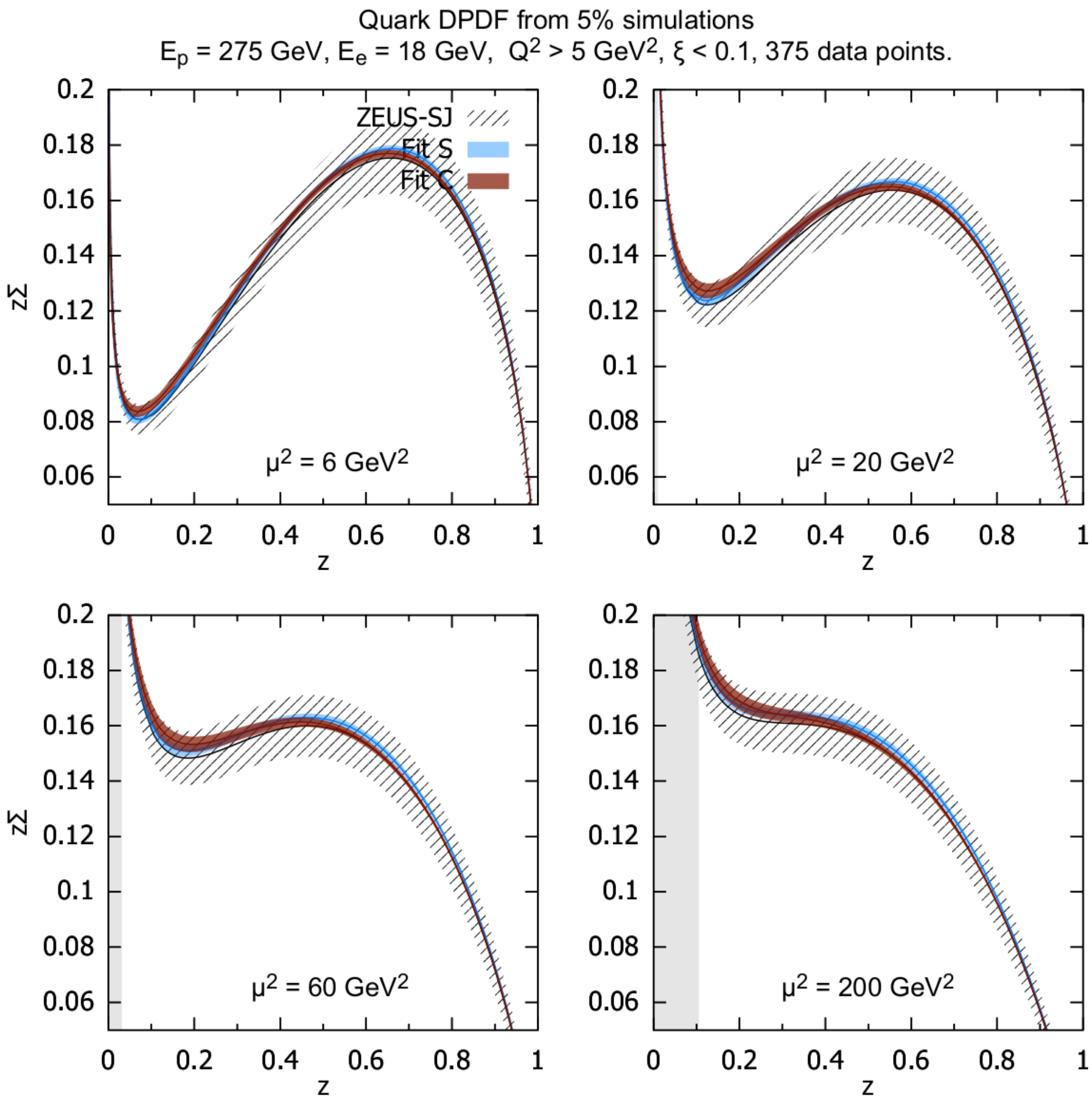

Data selection

$Q^2 > 5\ \mathrm{GeV}^2$

$\xi < 0.1$

- As compared to HERA
  - Higher accuracy
  - More data points

Sensitivity to the Reggeon contribution to σ_{red}

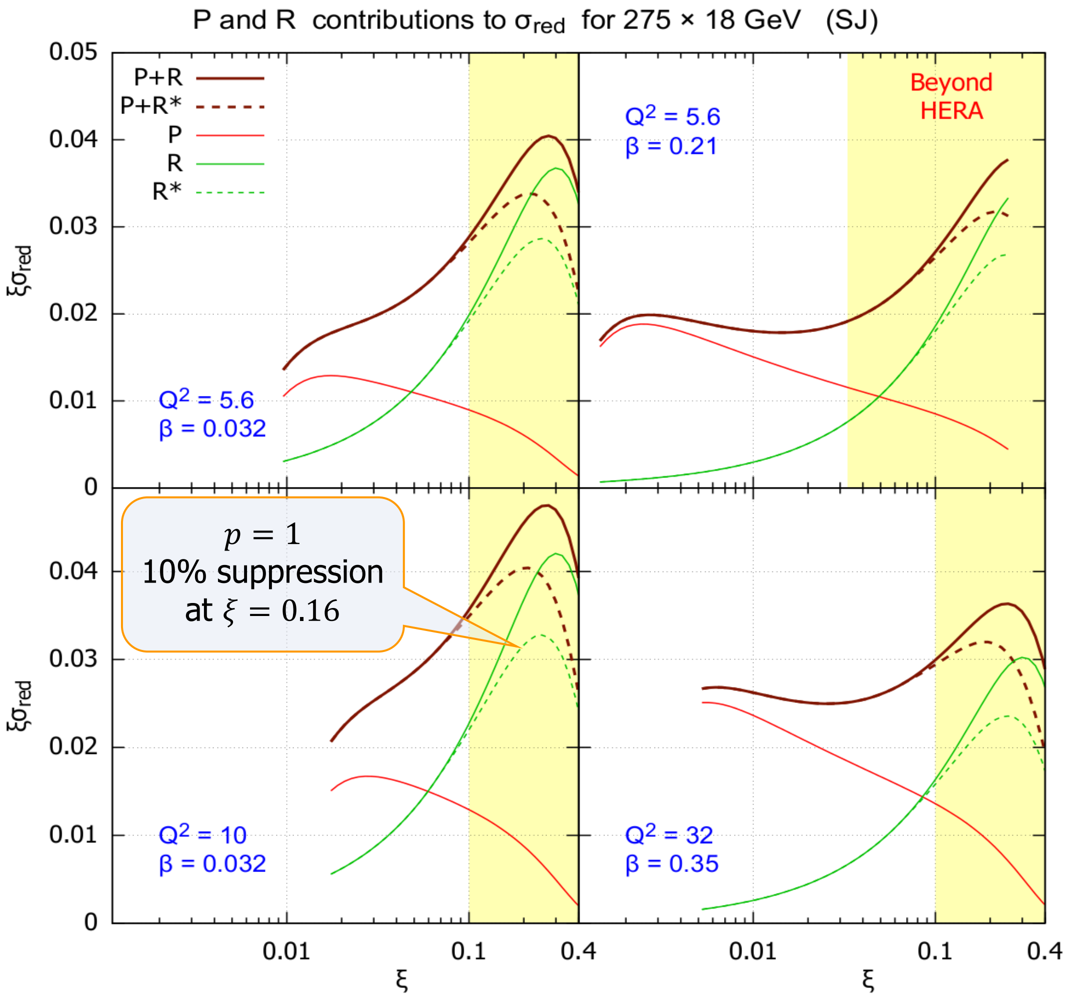

Procedure

1. Suppress Reggeon by a factor
$$\mathbb{R}^* = \left(\frac{1-\xi}{1-\xi_0}\right)^p \mathbb{R} \text{ for } \xi > \xi_0 = 0.07,$$
2. Generate pseudo-data with nominal and modified $\mathbb{R}$ contributions,
3. Fit DPDFs, using Reggeon flux $\varphi_R \propto \xi^{1-2\alpha_R}$ with α_R free.

Results

- ❑ Fits to the unmodified $\mathbb{R}$ result in $\chi^2 \approx 1$, as expected.
- ❑ Fits to $\mathbb{R}^*$ suppressed by ~10% give $\chi^2 \approx 1.2$

  This excludes a simple power-law shape in ξ.

Data at $\xi > 0.3$ desired for the subleading exchange study.

Example of F_L fits

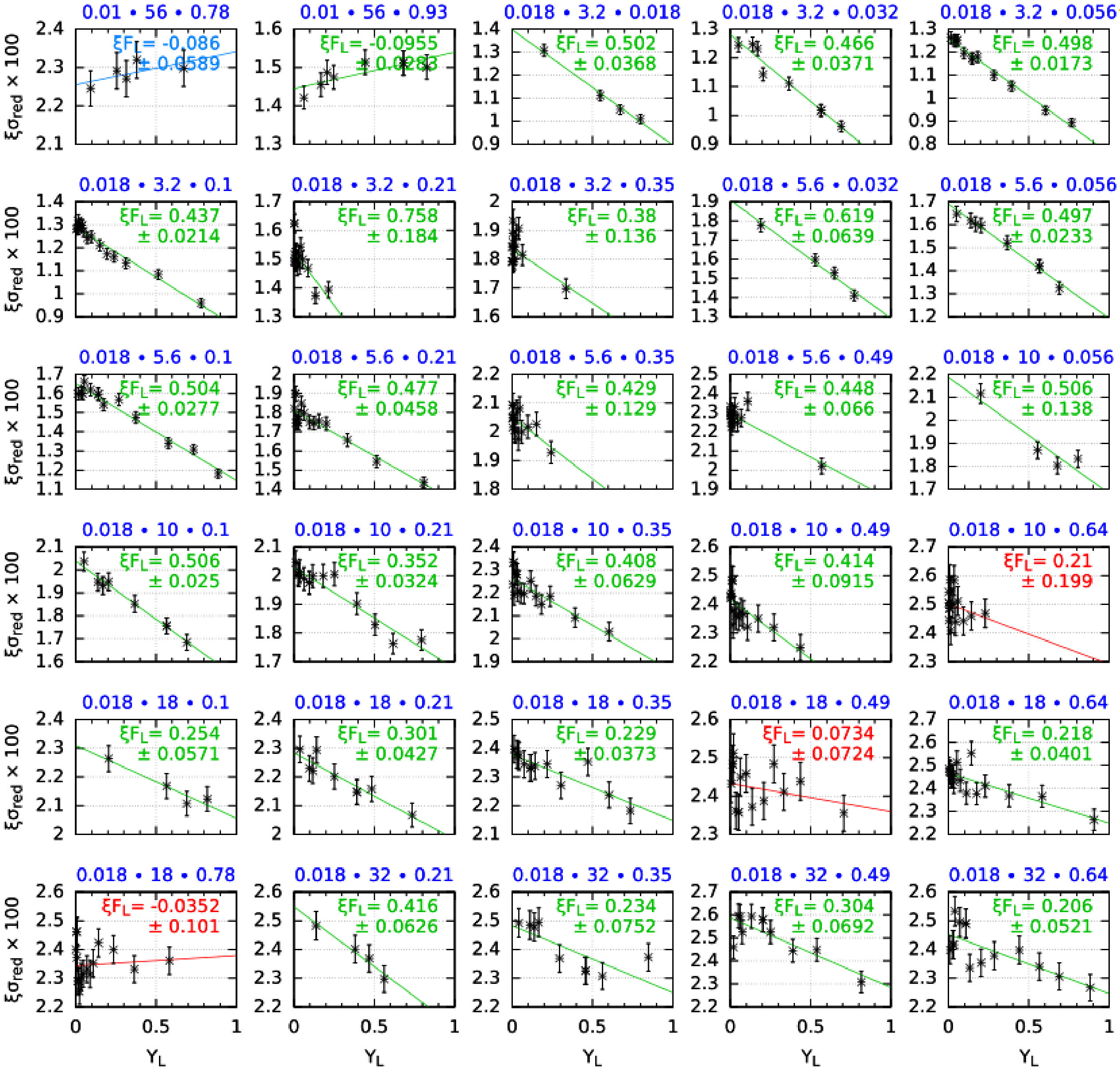

ξ, Q^2, β

$\delta_{sys} = 2\%$

$L = 10\ \mathrm{fb}^{-1}$

Simulated measurement of F_{L} vs. β in bins of (ξ, Q^2)

Example results of F_{L} fitted to $\sigma_{\mathrm{red}} = F_2 - Y_{\mathrm{L}}(y)\, F_{\mathrm{L}}$

76 bins in (ξ, Q^2)

F_L fit F_L model

First 20 of all 76 bins

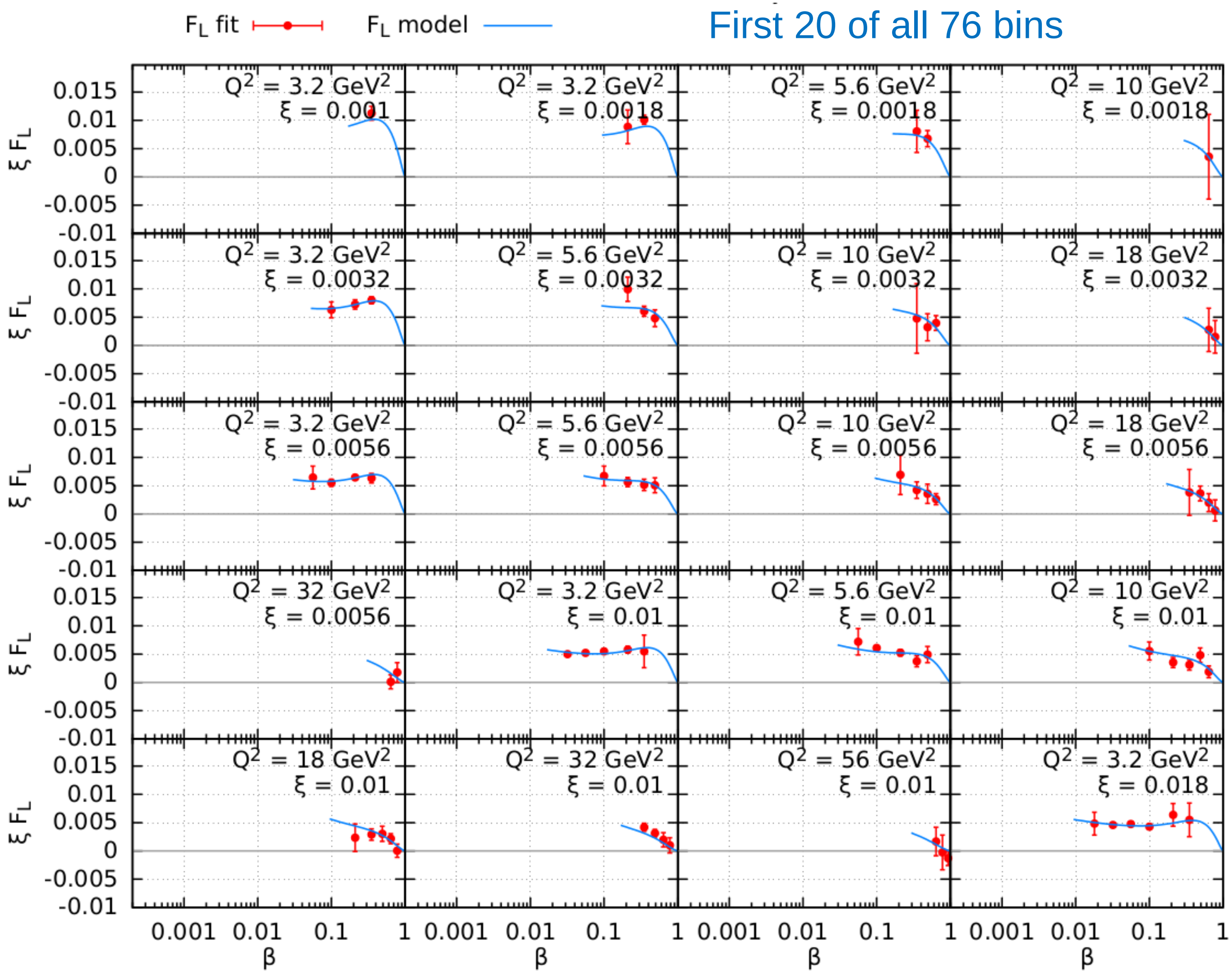

F_L fit

F_L model

Error bars correspond to the 90% confidence interval.

A reliable measurement of $F_{\mathrm{L}}^{\mathrm{D}(3)}$ within the reach of EIC

Simulated measurement of F_{L} vs. β in bins of (ξ, Q^2) (cont.)

Example results of F_{L} fitted to $\sigma_{\mathrm{red}} = F_2 - Y_{\mathrm{L}}(y)\, F_{\mathrm{L}}$

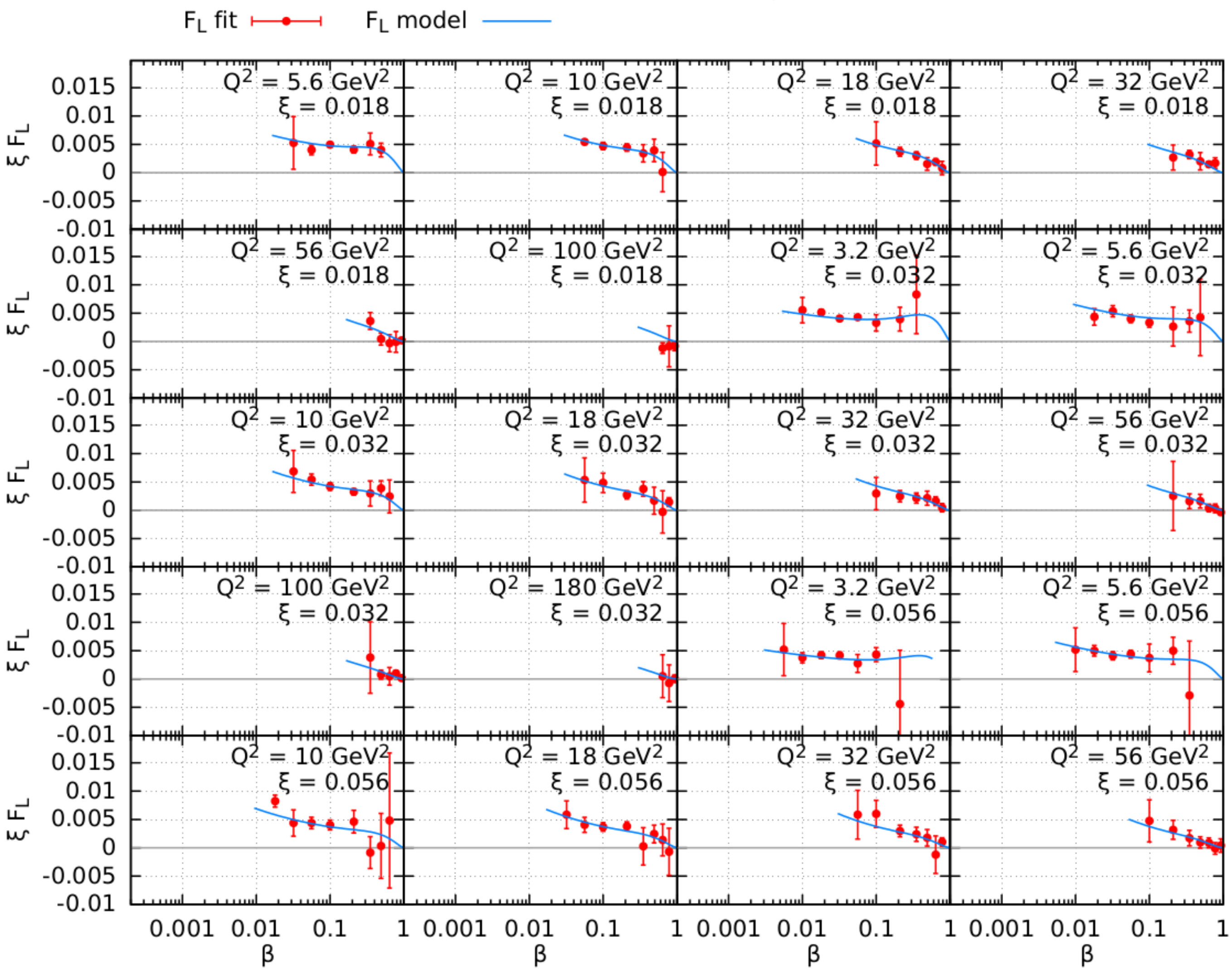

Next 20 of 76 bins in (ξ, Q^2)

F_{L} fit

F_{L} model

Error bars correspond to the 90% confidence interval.

A reliable measurement of $F_{\mathrm{L}}^{\mathrm{D}(3)}$ within the reach of EIC